Nanopore Current Oscillations: Nonlinear Dynamics on the Nanoscale

ARTICLE *in* JOURNAL OF PHYSICAL CHEMISTRY LETTERS · APRIL 2015

Impact Factor: 7.46 · DOI: 10.1021/acs.jpclett.5b00520

3 AUTHORS, INCLUDING:

Zuzanna Siwy

University of California, Irvine

151 PUBLICATIONS **6,257** CITATIONS

SEE PROFILE

Craig C Martens

University of California, Irvine

93 PUBLICATIONS **2,241** CITATIONS

SEE PROFILE

THE JOURNAL OF PHYSICAL CHEMISTRY Letters

Letter

pubs.acs.org/JPCL

Nanopore Current Oscillations: Nonlinear Dynamics on the Nanoscale

Brittany Hyland,[†] Zuzanna S. Siwy,[†,‡] and Craig C. Martens*[,†]

[†]Department of Chemistry, University of California—Irvine Irvine, California 92697-2025, United States

[‡]Department of Physics and Astronomy, University of California—Irvine Irvine, California 92697-4575, United States

ABSTRACT: In this Letter, we describe theoretical modeling of an experimentally realized nanoscale system that exhibits the general universal behavior of a nonlinear dynamical system. In particular, we consider the description of voltage-induced current fluctuations through a single nanopore from the perspective of nonlinear dynamics. We briefly review the experimental system and its behavior observed and then present a simple phenomenological nonlinear model that reproduces the qualitative behavior of the experimental data. The model consists of a two-dimensional deterministic nonlinear bistable oscillator experiencing both dissipation and random noise. The multidimensionality of the model and the interplay between deterministic and stochastic forces are both required to obtain a qualitatively accurate description of the physical system.

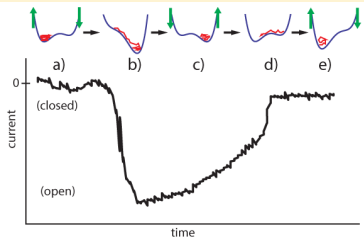

Two-mode nonlinear model of current oscillations

Nanopores are a subject of great current interest across a broad range of fields in engineering, physics, chemistry, and biology.[1−3] They serve both as simple models of biological pores and as potential new materials for transport and separation.[4−6]

In living systems, nanometer scale pores and channels control almost every physiological cellular function.[7,8] Both synthetic and biological nanopores are playing an increasingly important role in bionanotechnology as sensors for viruses, DNA, proteins, and other molecules.[9−18] Mimicking the voltage-responsive properties of biological channels in synthetic nanopores is especially useful, as voltage response provides rapid feedback.[19,20] In addition, voltage-controlled pores provide a basis for ionic circuits in biosensing, lab-on-a-chip, and artificial cell systems.[19]

In recent years, experiments on single nanopores have become possible, and they reveal a range of interesting phenomena associated with nonequilibrium transport, including rectification,[21−29] novel fluctuation statistics,[30−33] and nonlinear oscillations and bifurcation behavior.[34,35] Ion current oscillations have recently been observed in single conically shaped nanopores in our laboratory.[34,35] A similar effect of ion current instabilities was also observed in another nanopore system of nanopipettes.[36] The observed current time series in these systems are reminiscent of the oscillations of electrochemical processes at electrodes.[37,38] A general feature of electrodes exhibiting current oscillations is that they show a region of negative incremental resistance, or passivation, in their current−voltage curves; such behavior has also been observed recently in the current−voltage curves of conically shaped nanopores.[34,35]

The similarity of the oscillating waveforms across this diverse set of systems suggests the existence of an underlying universal mechanism.[37] Degn developed a mathematical model incorporating ideas from surface layer theory, including concentration polarization and overpotential,[37] whereas Koper et al. developed a model for oscillations and instabilities using an equivalent circuit[39−41] for cathodic systems. Koper, in particular, examined the connection between spontaneous oscillations and nonlinear dynamics.[41]

The theory of nonlinear dynamical systems provides a general framework for understanding, modeling, and predicting the complex behavior observed in fields spanning physical science, biology, engineering, medicine, and economics.[42−44] The exponential instability that can occur in nonlinear equations of motion, combined with dissipation, can lead to low dimensional chaotic dynamics, even in infinite dimensional systems. Chaos forms a paradigm of natural behavior that possesses both order and unpredictability. This unpredictability characterizing chaotic systems is deterministic, in contrast with statistical uncertainties typically represented as stochastic processes. Real systems can exhibit both chaos and noise in practice.

In this paper, we describe an experimentally realized nanoscale system that exhibits the general universal behavior of a nonlinear dynamical system, in particular, a nonlinear oscillator. First, we briefly review the experimental system and the behavior observed in the laboratory. We then present a simple phenomenological model that reproduces the qualitative behavior of the experimental system. The model consists of a two-dimensional deterministic nonlinear bistable oscillator experiencing both dissipation and random noise. The multidimensionality of the model and the interplay between

Received: March 11, 2015
Accepted: April 24, 2015
Published: April 24, 2015

   DOI: 10.1021/acs.jpclett.5b00520

deterministic and stochastic forces are both required to obtain a qualitatively accurate description of the physical system. The experimental system is reviewed below, and a simple phenomenological model that captures the qualitative behavior observed in the laboratory is described.

Experimental System. Recently, we reported the observation and analysis of ion current oscillations in a single conically shaped nanopore prepared in a polymer film.[34,35,45] In these experiments, the pore is in contact with a solution of weakly soluble salts, such as calcium hydrogen phosphate ($CaPHO_4$) or cobalt hydrogen phosphate ($CoHPO_4$), dissolved in a solution of 0.1 M KCl. Negative surface charges on the wall of the conical nanopore, combined with the externally applied voltage, lead to an increase of ionic concentrations within the pore, which in turn induces precipitation of the sparingly soluble components.[31,34] The precipitate is localized in the pore, possibly at its entrance, but not in the bulk, where the ionic concentrations do not exceed the solubility product.[46] In the measured current−voltage curves, the nanoprecipitation is observed as negative incremental resistance, a voltage range over which higher voltages produce lower average values of the current.[34,45] The precipitates are unstable and their dynamic formation and dissolution can be seen in the time domain as an alternating blocking and opening of the pores, respectively. This repeating process then leads to the observed current oscillations in time-dependent measurements.

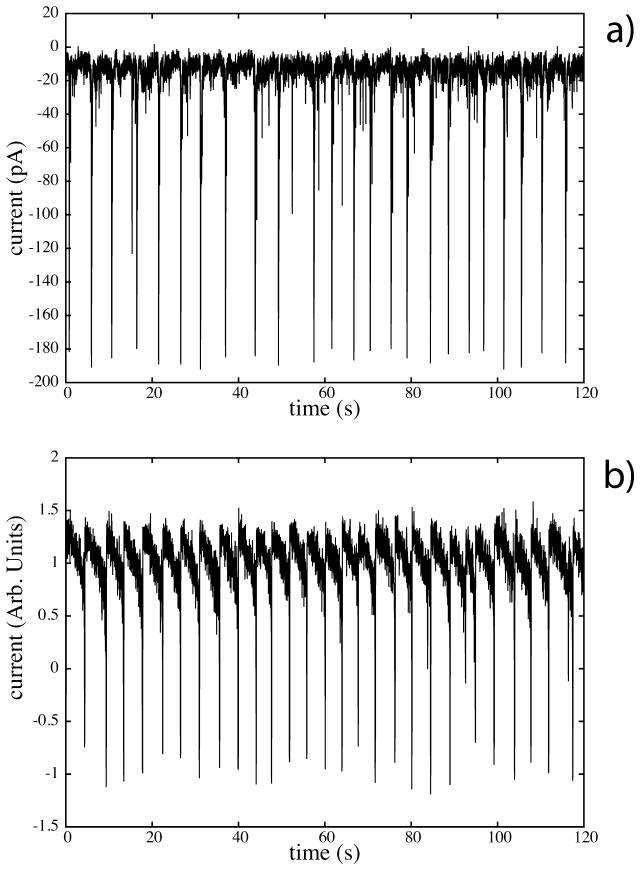

Figure 1. (a) Experimental current vs time measured for the single nanopore system with $V = -700$ mV over time interval of 120 s. The experiments were performed with a 6 nm in diameter single nanopore in 0.1 M KCl, 0.1 mM $CoCl_2$, and 2 mM PBS.[34] (b) Current time series predicted by the two mode nonlinear mode, as described in the text.

In the top panel of Figure 1 (labeled a), we show the experimental trace of current vs time for a single nanopore system with an applied voltage of −700 mV. For these conditions, the current exhibits bistability, with a closed state of nearly zero current interrupted by relatively short bursts of a larger (negative) current, corresponding to the open state. The behavior is roughly periodic, but there is variability in the times between the open states and in other structures of the time series. This behavior, somewhere between periodic and stochastic, suggests the possiblility of an underlying nonlinear dynamical mechanism.

In Figure 2a and c, we show magnifications of portions of the experimental current time series, encompassing the time scales of the period between pore openings and the opening event itself, respectively. The signals exhibit characteristic qualitative features, such as a relatively sharp opening, a slow subsequent current decrease, and then sudden closing. Our goal in the next section is to construct a nonlinear dyamical model of the qualitative and quantitative properties of this observed behavior.

The recordings of ion current as a function of time were analyzed using the commerical software Clampfit 9.2 (Molecular Devices, Inc.). Using built-in tools provided by the software, the events of pore openings and closings were found, as well as the duration of the subsequent open and closed states (dwell times). An opening event corresponds to a state with a high current level, compared to the ion current value recorded in 0.1 M KCl.[35] A closed state corresponded to low currents, typically close to −50 pA. Events were determined by defining the position of the baseline, the event line, and the rejection line (see Figure 1 of ref 35).

The average dwell times for the open and closed states are rather different, with the variability of the duration of the open states being smaller than the standard deviation of the closed state's dwell time. This suggests a deterministic mechanism of precipitate formation, which closes the pore.[35] The precipitation in a nanopore and the transition between high and low currents are related to the electric field induced flux of ions into and through the pore, which in turn determines the accumulation of sufficient ion concentration to form a precipitate.

Once the pore is closed, the voltage drop occurs primarily across the precipitate blockage, which is the component of the pore circuit with the highest resistance. Pore reopening can occur when the precipitate dissolves or is dislodged by electrophoretic or electroosmotic forces. In a negatively charged pore, for the voltage polarity at which cations are sourced from the narrow opening, concentrations of both cations and anions in the pore increase above the bulk concentrations. This is the polarity that promotes formation of precipitates. Once a precipitate is formed, it creates the highest resistance component in the system. As a result, the voltage drop across the remaining parts of the pore diminishes, which leads to lowering of local ionic concentrations, promoting the precipitate dissolution. These processes evidently contribute to the larger variation in the closed state dwell time.

In the case of precipitate dissolution, the variability can be explained as follows. The voltage drop is localized across the precipitate (before it has dissolved), which causes the solution adjacent to the precipitate to experience an electric field that alters the local ionic concentrations, diluting the solution

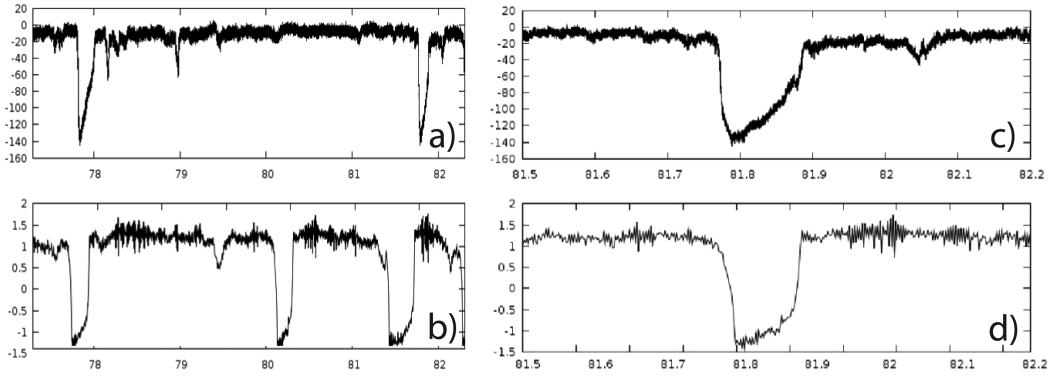

Figure 2. Comparison of time series for experimental data and two-dimensional model data. The experimental data and model results for an applied voltage of −700 mV on the time scale of interval between open pore events is given in (a) experiment and (b) model, respectively. The comparison between (c) experiment and (d) theory on time scale of the opening event is also shown. Parameters and scaling of the simulations are as described in the text.

around the blockage. The precipitate, thus, will be induced to dissolve and the pore will be reopen. It is expected that the time needed for the ionic concentrations to decrease and for the precipitate to dissolve will exhibit considerable variation depending on the details of its local structure. In the case of the precipitate being dislodged and expelled from the pore, the variability in the dwell time is also expected to be significant due to variability in its size, shape, and interaction with the pore surface.

Model. In this section, we describe a simple phenomenological two degree of freedom nonlinear oscillator model that qualitatively describes the time-dependent current of the single nanopore system. The model consists of two coupled modes (x,y) that evolve deterministically and are subjected to stochastic forces. The x degree of freedom represents the instantaneous current of the pore, whereas y represents a collective variable describing the involvement of additional internal degrees of freedom. The variables $x(t)$ and $y(t)$ obey the equations of motion

$$\dot{x} = -\frac{1}{\gamma_x}\frac{\partial U(x,y)}{\partial x} + f_x(t) \tag{1}$$

$$\dot{y} = \frac{1}{\gamma_y}[k_+H(x) - k_-H(-x)] + f_y(t) \tag{2}$$

The dynamics of $x(t)$ describes overdamped motion in a bistable well $U(x, y)$ which depends parametrically on the collective coordinate $y(t)$. The friction constant for x motion is given by γ_x. In addition to this deterministic overdamped motion, $x(t)$ is also under the influence of a random force $f_x(t)$. The dynamics of the collective coordinate $y(t)$ is characterized by simple time evolution that depends on the current state of the variable $x(t)$. We represent this behavior by assigning dy/dt a piecewise constant positive or negative value with magnitude k_+ or k_-, respectively, depending on the current state of the nanopore, reflected by the value of $x(t)$. In particular, the instantaneous rate selected depend on the sign of $x(t)$ through Heaviside function $H(x)$. The result is that $y(t)$ increases linearly with time with rate k_+ when $x(t)$ is positive, and decreases with rate k_- when $x(t)$ is negative. In addition, $y(t)$ is influenced by dissipation and noise with friction constant γ_y and random force $f_y(t)$, respectively. This phenomenological model introduces an x-state dependence on the behavior of $y(t)$ as simply as possible.

The bistable potential $U(x, y)$ is given by

$$U(x,y) = \frac{1}{4}ax^4 - \frac{1}{2}b(V)x^2 + cxy \tag{3}$$

The coupling term cxy between the x and y degrees of freedom determines the relative stabilities of the closed and open pore states, corresponding to the potential minima at negative and positive x values, respectively. The parameter c controls this coupling. The parameter $b(V)$ determines the general shape of the potential and, in particular, the absence or presence and height of the barrier at $x = 0$. For $b < 0$, a single (DC) current state at $x = 0$ is stable, whereas for $b > 0$ the system exhibits bistable open and closed current states. A bifurcation and thus change in behavior occurs at $b = 0$. The voltage dependence of parameter $b(V)$ is taken to be

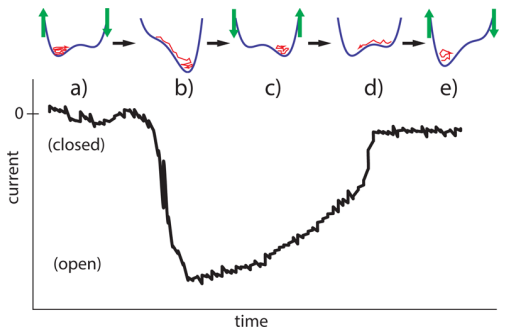

Figure 3. Schematic depiction of the evolution of the two mode nonlinear model and its relation to the measured current time series. Shown is a single experimental pore opening and reclosing event. (a) The stochastic trajectory $x(t)$ representing pore current is localized in the left well, corresponding to the low current (closed) state. In this state, $x < 0$, causing y to decrease according to eq 2. This causes the left well to raise in relation to the right, as indicated by the green arrows. (b) Eventually, the left well vanishes or becomes shallow enough for noise to induce the system to undergo a transition to the right well. This leads to an opening of the pore to the high (negative) current state. (c) In the open state, $x > 0$, causing y to increase. This causes a destabilization of the open state, as indicated by the green arrows. (d) Eventually, the well at positive x becomes shallow enough to allow a noise-induced transition to the now more stable closed state. (e) The process repeats itself. (Note that with our convention, a positive x corresponds to the open state, and thus a large but *negative* current.)

$$b(V) = b_0\left(\frac{V - V_c}{V_c}\right) \tag{4}$$

where V_c is the critical voltage. As the membrane voltage is increased through this value, the DC current becomes unstable, leading to the observed bistable behavior.

The differential equations are integrated using the Euler-Maruyama method for solving stochastic differential equations.[47] In the method, eqs 1 and 2 are discretized in time as

$$X_{n+1} = X_n - \frac{1}{\gamma_x}\frac{\partial U(X_n, Y_n)}{\partial x}\Delta t + \alpha\sqrt{\Delta t}\ W_{xn} \tag{5}$$

$$Y_{n+1} = Y_n + \frac{1}{\gamma_Y}[k_+H(X_n) - k_-H(-X_n)]\Delta t + \beta\sqrt{\Delta t}\ W_{yn} \tag{6}$$

where $X_n = x(n\Delta t)$, $Y_n = y(n\Delta t)$, with Δt the time step, (k_+, k_-) are the rates of switching between wells, (W_{xn}, W_{yn}) are a pair of normally distributed random numbers, and (α, β) are scale factors for the noise affecting the x and y modes, respectively.

In our numerical simulations, the potential parameters are taken to be $a = 1$, $b = 1$, and $c = 1$. The noise strength is $\alpha = \beta = 0.1$, whereas the damping parameters are $\gamma_x = 1$ and $\gamma_y = 100$. The rate parameters $k_+ = 1$ and $k_- = 5$; the relative magnitudes of these quantities determine the relative time spent in the open and closed states. With time scaling and current scaling, these generic and nonoptimized parameters give reasonable agreement between the model and experimental data.

There are several parameters in the model, but their relationships are constrained by the observed behavior of the experiment. The parameters of the potential $U(x,y)$ are all chosen to be unity, as this provides the universal and canonical bistable system. The variable $x(t)$ corresponds to the current, and comparison with experiment is accomplished by scaling. The barrier and relative well depths depend on $y(t)$, which evolves dynamically. Time scales of current fluctuations and transitions are determined by the value of the friction, which is chosen to be unity for the x motion, representing the current. Comparison with experiment then is accomplished by time scaling. The friction for the y motion is chosen to be 100. This choice is physically relevant, and establishes the overall rate of pore opening and closing in relation to the fluctuations and details of fast current changes. In spirit of a qualitative model, this number was not optimized by us beyond its order of magnitude, and leads to qualitative agreement with experiment. The choice of noise amplitude controls the magnitude of current fluctuations in relation to the absolute size of open and closed current states, as well as the distribution of transition times around the deterministically controlled mean. The value chosen was 0.1, again not optimized beyond its order of magnitude. These choices give qualitative agreement with experiment.

In Figure 3, we show a schematic illustration of the relation between the dynamics of the two mode nonlinear model and the experimental current time series. It should be noted that we take our open (high current) state to correspond to the minimum for $x > 0$, and our closed (low current) state as the minumum at $x < 0$. In the experiments, the open state corresponds to a high *negative* current, so a positive x in our model corresponds to a large but negative current in the experiment.

At state a, the stochastic trajectory $x(t)$ representing the pore current is fluctuating within the left well of the potential $U(x,y)$. This corresponds to the low current closed state of the nanopore. When the system is in this state, physical processes within the pore act to induce its opening. The corresponding evolution is captured in the nonlinear model through the phenomenonological collective variable $y(t)$. In the closed state, the current coordinate x is less than zero, causing y to decrease with time according to the equations of motion, eq 2. The shape of the potential $U(x,y)$ evolves such that the left well is raised in relation to the right, destabilizing the closed state, as indicated by the green arrows in the Figure. At (b), the left well has vanished or has become shallow enough for noise to induce a transition from the left well (closed state) to the right well (open state), corresponding to a transition in the time series from the low to the high (negative) current state. At (c), system is in the open state. Here, the physical process of precipitation of insoluble calcium salts act to cause the pore to reclose. In the model, $x > 0$ in the open state, causing y to increase through the equations of motion, which represents the precipitation and pore closure, as indicated by the green arrows. Eventually, the well at positive x becomes shallow enough to allow a noise-induced transition to the now more stable closed state, as indicated at (d). Once in the closed state, the cycle repeats itself, as denoted by the schematic diagram at (e).

Our multidimensional model allows the character of the bistable well to evolve in time through its coupling to a second, deterministic, degree of freedom. A relatively low level of noise can then promote transitions between the bistable current states when the barrier is lowered via deterministic dynamics, giving a roughly periodic dependence with a random fluctuation of opening and closing times around a mean. This is the behavior observed in the experiment. For a one-dimensional model, the bistable well is static, and noise must do the entire job of promoting transitions over that fixed height barrier. The result is very noisy transitions with ill-defined period. This highly random behavior is a consequence of the lower dimensionality and is inconsistent with experiment.

Results. Figure 1 shows a comparison of the experimental time series with the predictions of the nonlinear model. The experimental data is presented in the top panel, labeled a, as described above, whereas the theoretical results is given in the bottom panel, labeled b. The roughly periodic nature of the pore opening and closing and the fractions of time the pore is in the open and closed states are qualitatively captured by the model. The gross agreement of time scales is obtained by adjusting the dimensionless model parameters and scaling the time of the theoretical results to fit the average frequency of events of the experimental data. Beyond that, the agreement with the qualitative appearance and the more quantitative statistical measures provide a test of the form and parameters of the model. The relative open and closed times is controlled by the relative magnitudes of k_+ and k_-, whereas the variability of the open and closed intervals depends on the values of the corresponding noise amplitude and friction. The current values of the model data are left in dimensionless units, so only a qualitative comparison can be made.

In Figure 2, comparison between model and experiment is made on the shorter time scales of individual events and the intervals between them. The qualitative agreement is again seen to be good; both the real data and the model data have the same general characteristics: an initial region of steep increase in the negative current, followed by a small region of gradual

DOI: 10.1021/jz500530

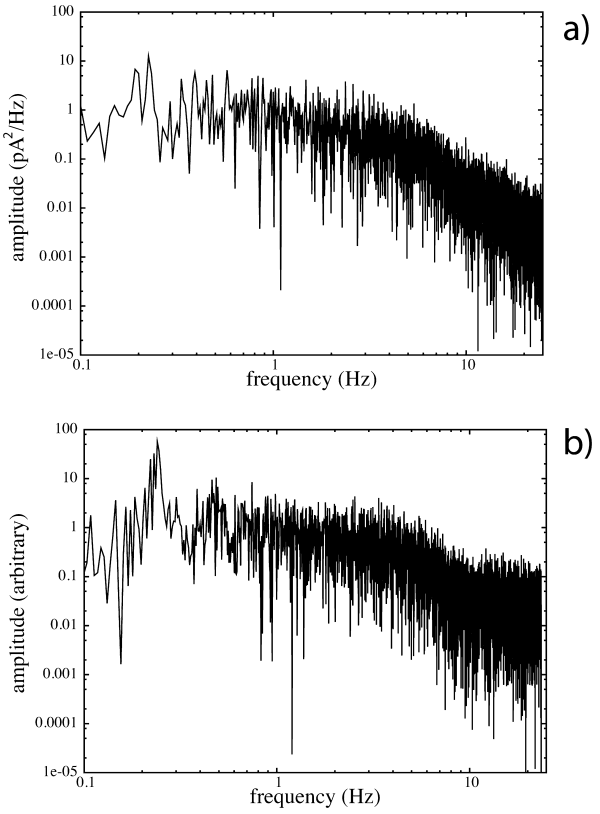

Figure 4. Power series comparison between data collected at −700 mV (a, top) and 2D model (b, bottom), as described in the text.

change, and finally, a region of steep return to the low current closed state. The similarity in behavior between our two-dimensional nonlinear stochastic simulation and the experimental time series suggests that the model captures the essense of the underlying dynamical processes.

Further comparison can be made by calculating spectral and statistical properties of the experimental data and comparing them with predictions of the theoretical model. In Figure 4, the power spectrum of the experimental and model time series are compared, again for the case of $V = -700$ mV. In both the experiment and the model, the power spectrum has a feature at low frequency that is related to the approximate periodicity of the time series. The peak center and width of the model are in good agreement, indicating that the variability of opening times are qualitatively captured by the model (the time scaling ensures that the peak centers agree). In addition, the falloff of the log spectra for the experimental and theoretical data with increasing frequency are qualitatively similar, indicating that the nonlinear stochastic model reproduces the scaling of both the individual opening event statistics and the noise properties as frequency increases.

A more detailed comparison can be made by computing the statistics of the dwell times for the closed and open states, respectively. The probability distribution of times, $P(T)$ vs the dwell times T are presented in Figure 5. Again, the agreement is not quantitative, but is reasonable, given the simplicity of the model. In particular, both the mean values and the variability of the opening and closing events are captured by the model. These results are characterized by distributions with fairly well-defined open and closed dwell times, leading to relatively sharp peaks with wide but low tails. A simpler model of stochastic overdamped motion in a one-dimensional bistable well yields

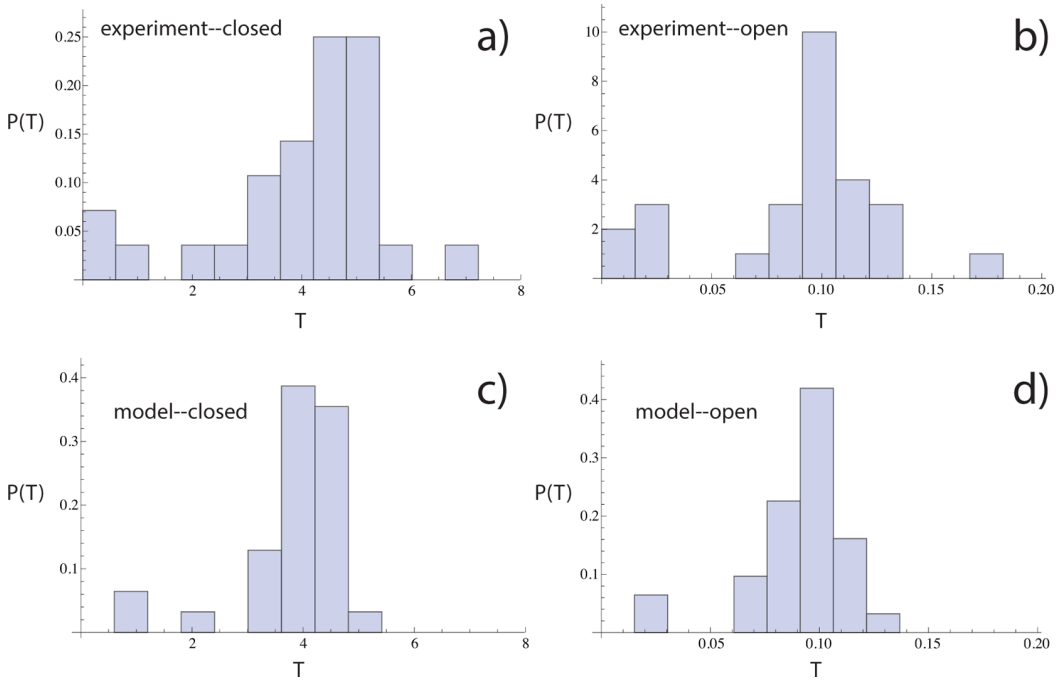

Figure 5. Comparison of closed and open dwell time probability distributions $P(T)$ for experimental data (top row) collected at −900 mV and model data (bottom row). The experiments were performed with a 6 nm in diameter single nanopore in 0.1 M KCl, 0.1 mM $CoCl_2$, and 2 mM PBS.[34] Dwell times T are given in seconds, and the dimensionless model data times are scaled as described in text. (a) Experimental distribution of closed times. (b) Experimental distribution of open times. (c) Model predictions of distribution of closed times. (d) Model prediction of distribution of open times.

far broader distributions and far more aperiodic time series. The multidimensionality of the nonlinear oscillator is essential to achieve this level of agreement.

Conclusion. In this paper, we have proposed a two-dimensional nonlinear phenomenological model to describe, in as simple but qualitatively correct a manner as possible, the behavior of the single nanopore oscillator system studied experimentally by Siwy and co-workers.[34,35,45] A one-dimensional nonlinear stochastic model cannot capture even the qualitative behavior of pore opening and closing observed in the experimental system, and two coupled deterministic degrees of freedom influenced by stochastic forces are the simplest conditions leading to a successful model. In addition, both nonlinearity and noise are required to obtain the observed qualitative behavior. A fully deterministic nonlinear model does not lead to the observed variability in the open and closed state dwell times. This is reminiscent of the Brownian motor paradigm used to describe molecular machines, where noise is an essential part of their function.[48] This is in contrast with previously studied macroscopic electrochemical oscillators, which can be modeled by deterministic nonlinear differential equations. At the nanoscale, fluctuations take on an increasingly important role, and a combination of noise and determinism are needed to understand and model nanopore current oscillations.

AUTHOR INFORMATION

Corresponding Author

*E-mail: cmartens@uci.edu.

Notes

The authors declare no competing financial interest.

ACKNOWLEDGMENTS

This work was supported by the National Science Foundation.

REFERENCES

(1) Howorka, S.; Siwy, Z. Nanopore Analytics: Sensing of Single Molecules. *Chem. Soc. Rev.* **2009**, *38*, 2360−2384.

(2) *Nanopores: Sensing and Fundamental Biological Interactions*; Iqbal, S., Bashir, R., Eds.; Springer: Berlin, 2011.

(3) Gracheva, M. E. *Nanopore-Based Technology*; Methods in Molecular Biology; Humana Press: New York, 2012.

(4) Schoch, R.; Han, J.; Renaud, P. Transport Phenomena in Nanofluidics. *Rev. Mod. Phys.* **2008**, *80*, 839−883.

(5) Lev, A. A.; Korchev, Y. E.; Rostovtseva, T. K.; Bashford, C. L.; Edmonds, D. T.; Pasternak, C. A. Rapid Switching of Ion Current in Narrow Pores - Implications for Biological Ion Channels. *Proc. R. Soc. B* **1993**, *252*, 187−192.

(6) Siwy, Z.; Fuliński, A. Origin of $1/f^{\alpha}$ Noise in Membrane Channel Currents. *Phys. Rev. Lett.* **2002**, *89*, 158101.

(7) Cooper, G. M. *The Cell−A Molecular Approach*; Sinauer Associates, Sunderland, MA, 2000.

(8) Hille, B. *Ion Channels of Excitable Membranes*; Sinauer Associates: Sunderland, MA, 2001.

(9) Kasianowicz, J.; Brandin, E.; Branton, D.; Deamer, D. Characterization of Individual Polynucleotide Molecules Using a Membrane Channel. *Proc. Natl. Acad. Sci. U.S.A.* **1996**, *93*, 13770−13773.

(10) Bayley, H.; Martin, C. Resistive-Pulse Sensing — From Microbes to Molecules. *Chem. Rev.* **2000**, *100*, 2575−2594.

(11) Henriquez, R. R.; Ito, T.; Sun, L.; Crooks, R. M. The Resurgence of Coulter Counting for Analyzing Nanoscale Objects. *Analyst* **2004**, *129*, 478.

(12) Venkatesan, B. M.; Bashir, R. Nanopore Sensors for Nucleic Acid Analysis. *Nat. Nanotechnol.* **2011**, *6*, 615−624.

(13) Cherf, G. M.; Lieberman, K. R.; Rashid, H.; Lam, C. E.; Karplus, K.; Akeson, M. Automated Forward and Reverse Ratcheting of DNA in a Nanopore at 5-Å Precision. *Nat. Biotechnol.* **2012**, *30*, 344−348.

(14) Manrao, E. A.; Derrington, I. M.; Laszlo, A. H.; Langford, K. W.; Hopper, M. K.; Gillgren, N.; Pavlenok, M.; Niederweis, M.; Gundlach, J. H. Reading DNA at Single-Nucleotide Resolution with a Mutant MspA Nanopore and Phi29 DNA Polymerase. *Nat. Biotechnol.* **2012**, *30*, 349−353.

(15) Movileanu, L. Squeezing a Single Polypeptide Through a Nanopore. *Soft Matter* **2008**, *4*, 925.

(16) Deblois, R. W.; Bean, C. P.; Wesley, R. K. Electrokinetic Measurements with Submicron Particles and Pores by the Resistive Pulse Technique. *J. Colloid Interface Sci.* **1977**, *61*, 323−335.

(17) DeBlois, R. W. Counting and Sizing of Submicron Particles by the Resistive Pulse Technique. *Rev. Sci. Instrum.* **1970**, *41*, 909.

(18) Harms, Z. D.; Mogensen, K. B.; Nunes, P. S.; Zhou, K.; Hildenbrand, B. W.; Mitra, I.; Tan, Z.; Zlotnick, A.; Kutter, J. P.; Jacobson, S. C. Nanofluidic Devices with Two Pores in Series for Resistive-Pulse Sensing of Single Virus Capsids. *Anal. Chem.* **2011**, *83*, 9573−9578.

(19) Siwy, Z.; Howorka, S. Engineered Voltage-Responsive Nanopores. *Chem. Soc. Rev.* **2010**, *39*, 1115.

(20) Powell, M. R.; Cleary, L.; Davenport, M.; Shea, K. J.; Siwy, Z. S. Electric-Field-Induced Wetting and Dewetting in Single Hydrophobic Nanopores. *Nat. Nanotechnol* **2011**, *6*, 798−802.

(21) Wei, C.; Bard, A. J.; Feldberg, S. W. Current Rectification at Quartz Nanopipet Electrodes. *Anal. Chem.* **1997**, *69*, 4627−4633.

(22) Siwy, Z.; Spohr, H. A.; Baur, D.; Wolf-Reber, A.; Spohr, R.; Apel, P.; Korchev, Y. E. Rectification and Voltage Gating in Ion Currents in a Nanofabricated Pore. *Europhys. Lett.* **2002**, *60*, 349−355.

(23) Daiguji, H.; Oka, Y.; Shirono, K. Nanofluidic Diode and Bipolar Transistor. *Nano Lett.* **2005**, *5*, 2274−2280.

(24) Siwy, Z. Ion-Current Rectification in Nanopores and Nanotubes with Broken Symmetry. *Adv. Funct Mater.* **2006**, *16*, 735−746.

(25) Cervera, J.; Schiedt, B.; Neumann, R.; Mafe, S.; Ramirez, P. Ionic Conduction, Rectification, and Selectivity in Single Conical Nanopores. *J. Chem. Phys.* **2006**, *124*, 104706.

(26) He, Y.; Gillespie, D.; Boda, D.; Vlassiouk, I.; Eisenberg, R. S.; Siwy, Z. S. Tuning Transport Properties of Nanofluidic Devices with Local Charge Inversion. *J. Am. Chem. Soc.* **2009**, *131*, 5194−5202.

(27) White, H. S.; Bund, A. Ion Current Rectification at Nanopores in Glass Membranes. *Langmuir* **2008**, *24*, 2212−2218.

(28) Yameen, B.; Ali, M.; Neumann, R.; Ensinger, W.; Knoll, W.; Azzaroni, O. Single Conical Nanopores Displaying pH-Tunable Rectifying Characteristics. Manipulating Ionic Transport With Zwitterionic Polymer Brushes. *J. Am. Chem. Soc.* **2009**, *131*, 2070−2071.

(29) Sa, N.; Fu, Y.; Baker, L. A. Reversible Cobalt Ion Binding to Imidazole-Modified Nanopipettes. *Anal. Chem.* **2010**, *82*, 9963−9966.

(30) Smeets, R. M. M.; Keyser, U. F.; Dekker, N. H.; Dekker, C. Noise in Solid-State Nanopores. *Proc. Natl. Acad. Sci. U.S.A.* **2008**, *105*, 417−421.

(31) Powell, M. R.; Vlassiouk, I.; Martens, C.; Siwy, Z. S. Nonequilibrium $1/f$ Noise in Rectifying Nanopores. *Phys. Rev. Lett.* **2009**, *103*, 248104.

(32) Powell, M. R.; Martens, C.; Siwy, Z. S. Asymmetric Properties of Ion current $1/f$ Noise in Conically Shaped Nanopores. *Chem. Phys.* **2010**, *375*, 529−535.

(33) Powell, M. R.; Sa, N.; Davenport, M.; Healy, K.; Vlassiouk, I.; Letant, S. E.; Baker, L. A.; Siwy, Z. S. Noise Properties of Rectifying Nanopores. *J. Phys. Chem. C* **2011**, *115*, 8775−8783.

(34) Powell, M. R.; Sullivan, M.; Vlassiouk, I.; Constantin, D.; Sudre, O.; Martens, C. C.; Eisenberg, R. S.; Siwy, Z. S. Nanoprecipitation-Assisted Ion Current Oscillations. *Nat. Nanotechnol* **2008**, *3*, 51−57.

(35) Inness, L.; Powell, M. R.; Vlassiouk, I.; Martens, C.; Siwy, Z. S. Precipitation-Induced Voltage-Dependent Ion Current Fluctuations in Conical Nanopores. *J. Phys. Chem. C* **2010**, *114*, 8126−8134.

(36) Yusko, E. C.; Billeh, Y. N.; Mayer, M. Current Oscillations Generated by Precipitate Formation in the Mixing Zone Between Two

Solutions Inside a Nanopore. *J. Phys.: Condens. Matter* **2010**, *22*, 454127.
(37) Degn, H. Theory of Electrochemical Oscillations. *Trans. Faraday Soc.* **1968**, *64*, 1348−1358.
(38) Franck, U.; FitzHugh, R. *Z. Elektrochem.* **1961**, *65*, 156.
(39) Koper, M.; Sluyters, J. Electrochemical Oscillators: Their Description Through a Mathematical Model. *J. Electroanal. Chem.* **1991**, *303*, 73−94.
(40) Koper, M.; Gaspard, P. The Modelling of Mixed-Mode and Chaotic Oscillations in Electrochemical Systems. *J. Phys. Chem.* **1992**, *96*, 7797−7813.
(41) Koper, M. Non-Linear Phenomena in Electrochemical Systems. *J. Chem. Soc., Faraday Trans.* **1998**, *94*, 1369−1378.
(42) Kaplan, D.; Glass, L. *Understanding Nonlinear Dynamics*; Springer: Berlin, 1995.
(43) Wiggins, S. *Introduction to Applied Nonlinear Dynamical Systems and Chaos*; Springer: Berlin, 2003.
(44) Strogatz, S. H. *Nonlinear Dynamics and Chaos, With Applications to Physics, Biology Chemistry, and Engineering*; Westview Press: Boulder, CO, 2014.
(45) Siwy, Z. S.; Powell, M. R.; Petrov, A.; Kalman, E.; Trautmann, C.; Eisenberg, R. *Nano Lett.* **2006**, *6*, 1729.
(46) Cruz-Chu, E. R.; Schulten, K. Computational Microscopy of the Role of Protonable Surface Residues in Nanoprecipitation Oscillations. *ACS Nano* **2010**, *4*, 4463−4474.
(47) Kloeden, P. E.; Platen, E. *Numerical Solution of Stochastic Differential Equations*; Springer, Berlin, 1999.
(48) Reimann, P. Brownian Motors: Noisy Transport Far From Equilibrium. *Phys. Rep.* **2002**, *361*, 57265.